Preparation and reactivity of metal-containing monomers
41.* The formation and thermal transformations of nanometer-sized particles of cobalt ferrite upon the decomposition of coprecipitated Fe^{III} and Co^{II} acrylates

*A. S. Rozenberg, E. I. Aleksandrova, G. I. Dzhardimalieva, N. V. Kir'yakov, P. E. Chizhov, V. I. Petinov, and A. D. Pomogailo**

Institute of Chemical Physics in Chernogolovka, Russian Academy of Sciences, 142432 Chernogolovka, Moscow Region, Russian Federation. Fax: +7 (096) 515 3588

Thermal transformations (at 340 to 390 °C) of coprecipitates of iron and cobalt acrylates, $[Fe_3O(CH_2CHCOO)_6OH][Co(CH_2CHCOO)_2]_{2.4}$ (**1**) and $[Fe_3O(CH_2CHCOO)_6OH][Co(CH_2CHCOO)_2]_{1.5} \cdot 3H_2O$ (**2**), are studied. The dependence of the degree of gas evolution (η) on time is described by the equation $\eta(t) = \eta_{1\infty}[1 - \exp(-k_1\tau)] + (1 - \eta_{1\infty})[1 - \exp(-k_2\tau)]$, where $k_1 = 2.3 \cdot 10^{12} \cdot \exp[-49500/(RT)]$ s^{-1}, $k_2 = 6.0 \cdot 10^6 \cdot \exp[-33000/(RT)]$ s^{-1} and $k_1 = 2.6 \cdot 10^{12} \cdot \exp[-49000/(RT)]$ s^{-1}, $k_2 = 6.6 \cdot 10^5 \cdot \exp[-30000/(RT)]$ s^{-1} for cocrystallizates **1** and **2**, respectively. The coefficient $\eta_{1\infty}$ decreases as the temperature increases. The value of $\eta_{1\infty}$ for compound **1** is higher than that for compound **2**. The composition of products of the transformations of **1** and **2** are studied. The main solid state products of the decomposition are nanometer-sized particles of cobalt ferrite, $CoFe_2O_4$, with a narrow size distribution stabilized by the polymeric matrix. The thermal transformations of cocrystallizates **1** and **2** include dehydration, thermal decomposition, copolymerization in the solid state, and decarboxylation of the metallocarboxylate groups of the polymer. The effect of the ratio between the Fe clusters and the Co-containing fragments on the process of thermal transformation is analyzed.

Key words: iron and cobalt acrylates, trinuclear iron cluster, ultradispersed cobalt ferrite; solid state polymerization.

Thermal transformations of acrylates of transition metals, including those with cluster structures, occur through two main processes:[1–3] solid-state polymerization of the initial monomer and decarboxylation of the metallocarboxylate groups in the metallopolymer formed followed by the isolation of the metal or its oxide as ultradispersed particles. The thermal transformation of metal acrylates is the only process known at the present time (*cf.* Refs. 4 and 5) that allows one to simultaneously synthesize ultradispersed particles and chemically passivate them, thus solving one of the current problems of physical chemistry of the ultradispersed state.[6]

The results of the study of thermal transformations in the $[Fe_3O(CH_2CHCOO)_6OH][Co(CH_2CHCOO)_2]_{2.4}$ (**1**) and $[Fe_3O(CH_2CHCOO)_6OH][Co(CH_2CHCOO)_2]_{1.5} \cdot 3H_2O$ (**2**) systems in which the atomic ratios Fe : Co are close to 1 : 0.8 and 2 : 1, respectively, are presented in this work. This study is of interest from the viewpoint of the mutual effect of metallomonomers of different natures (whose independent behavior has previously been studied[1,3]) on the processes of thermal transformation in their mixtures and because of the possibility of synthesizing complex metal oxides (ferrites) in the polymer matrix. The thermal decomposition of mixtures of acrylates of two different metals has not been studied to date.

Kinetic regularities of the thermal transformation of cocrystallizates 1 and 2. The thermal transformations of compounds **1** and **2** are accompanied by gas evolution at experimental temperatures (T_{exp}) from 340 to 390 °C. This is preceded by noticeable gas evolution during heating of the sample (~3 min): $\alpha_n^{\Sigma} = 0.42$ (**1**), 0.35 (**2**) (where α_n^{Σ} is the number of moles of gaseous products evolved per 1 mole of the initial substance). Then the rate of gas evolution decreases. The dependence of the degree of gas evolution (η) on time (Fig. 1) in the case of cocrystallizates **1** and **2** is described by an equation for two parallel reactions:

$$\eta(t) = \eta_{1\infty}[1-\exp(-k_1\tau)] + (1-\eta_{1\infty})[1-\exp(-k_2\tau)],$$

where $\eta = \alpha_t^{\Sigma}/\Delta\alpha_{\infty}^{\Sigma}$ is the degree of gas evolution; $\Delta\alpha_t^{\Sigma} = \alpha_t^{\Sigma} - \alpha_n^{\Sigma}$, $\Delta\alpha_{\infty}^{\Sigma} = \alpha_{\infty}^{\Sigma} - \alpha_n^{\Sigma}$, α_t^{Σ} and α_{∞}^{Σ} are the current and final numbers of moles, respectively; $\eta_{1\infty} = (\alpha_{\infty}^{\Sigma} - \alpha_n^{\Sigma})/(\Delta\alpha_{\infty}^{\Sigma})$; $\tau = t - t_n$, t_n is the time of heating; k is the effective rate constant. The values of $\Delta\alpha_{\infty}^{\Sigma}$, k, and $\eta_{1\infty}$ depend on T_{exp}.

* For Part 40, see *Russ. Chem. Bull.*, 1994, **43**, 2020.

Translated from *Izvestiya Akademii Nauk. Seriya Khimicheskaya,* No. 5, pp. 885—893, May, 1995.

1066-5285/95/4405-0858 $12.50

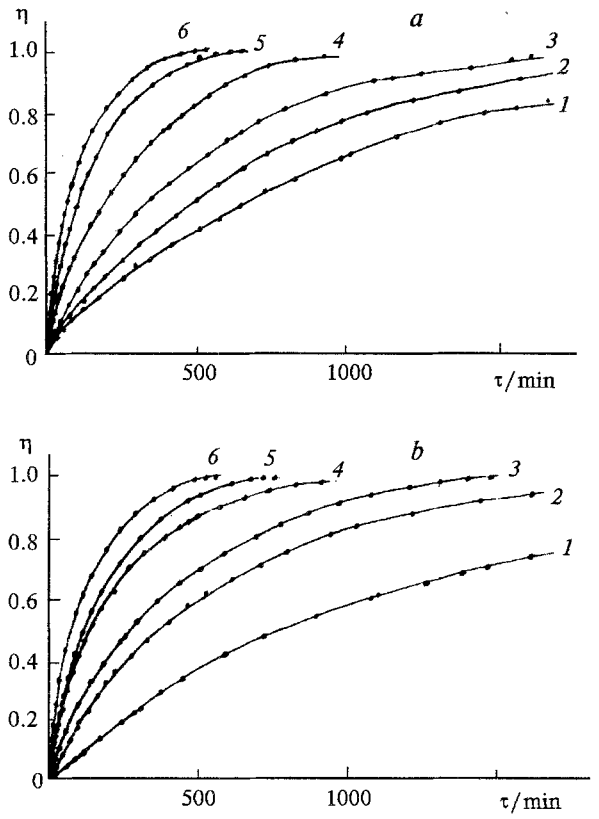

Fig. 1. Kinetics of the accumulation of gaseous products in the thermal transformation of cocrystallizates **1** (*a*) and **2** (*b*). Curves present the calculations according to Eq. (1), dots present the experimental values: T_{exp} = 340 °C (*1*); 350 °C (*2*); 360 °C (*3*); 370 °C (*4*); 380 °C (*5*); 390 °C (*6*); m_0/V = $1.28 \cdot 10^{-3}$ g cm^{-3} (**1**) and $1.80(\pm 0.05) \cdot 10^{-3}$ g cm^{-3} (**2**).

For cluster **1**, when T_{exp} increases, the value of $\eta_{1\infty}$ decreases from 0.65 at 340 °C to 0.45 at 370 to 390 °C,

$$k_1 = 2.3 \cdot 10^{12} \cdot \exp[-(49500 \pm 2500)/(RT)] \text{ s}^{-1},$$

$$k_2 = 6.0 \cdot 10^{6} \cdot \exp[-(33000 \pm 2000)/(RT)] \text{ s}^{-1},$$

$$\alpha_\infty^{\Sigma} = 5.25 \cdot 10^{2} \cdot \exp[-(7500 \pm 1000)/(RT)].$$

For cluster **2**, when T_{exp} increases, $\eta_{1\infty}$ decreases from 0.5 at 340 °C to 0.35 at 370 to 390 °C,

$$k_1 = 2.6 \cdot 10^{12} \cdot \exp[-(49000 \pm 2500)/(RT)] \text{ s}^{-1},$$

$$k_2 = 6.6 \cdot 10^{5} \cdot \exp[-(30000 \pm 2000)/(RT)] \text{ s}^{-1},$$

$$\alpha_\infty^{\Sigma} = 1.90 \cdot 10^{2} \cdot \exp[-(6000 \pm 1000)/(RT)] \text{ s}^{-1}.$$

The temperature dependences of k_1, k_2, and $\Delta\alpha_\infty^{\Sigma}$ are similar for compounds **1** and **2**. It is noteworthy that the value of k_2 is comparable to the effective rate constant of the thermal transformation of $Fe_3O(CH_2CHCOO)_6OH \cdot 3H_2O$ (**3**), which is equal to $1.3 \cdot 10^{6} \cdot \exp[-30500/(RT)]$ s^{-1} in this temperature range, while k_1 is lower than the rate constant of the decomposition of $Co(CH_2CHCOO)_2 \cdot H_2O$ [1] (**4**) and the rate constant for the decomposition of **3** in the 200 to 300 °C temperature range (*cf.* Ref. 3).

At the same time, the values of $\eta_{1\infty}$ for **1** are higher than those for **2**. No effects of the ratio m_0/V (where m_0 is the mass of the initial sample, V is the volume of the reaction vessel) on the kinetics of the transformations of cocrystallizates **1** and **2** are observed.

The composition of the products of the transformations of cocrystallizates 1 and 2. *Gaseous and condensing products.* According to the data of IR spectroscopy and mass spectrometry, CO_2 is the main gaseous product in the T_{exp} range studied, and H_2 and CO evolve in substantially smaller amounts. The vapor of acrylic acid, $CH_2CHCOOH$, and H_2O also exist in the gaseous products. They condense on the cool parts of the reaction vessel in the process of heating the sample to T_{exp}.

The amount of CO_2 (α_{CO_2}) observed at the end of the transformation increases as T_{exp} increases:

$$(\alpha_{CO_2})_1 = 0.43 \cdot 10^{2} \cdot \exp[-(4700 \pm 500)/(RT)],$$

$$(\alpha_{CO_2})_2 = 0.41 \cdot 10^{2} \cdot \exp[-(4500 \pm 500)/(RT)].$$

The total yield of CO_2 and CO ($\alpha_{CO_2} + \alpha_{CO}$) also increases at the end of the transformation as T_{exp} increases:

$$(\alpha_{CO_2} + \alpha_{CO})_1 = 1.3 \cdot 10^{2} \cdot \exp[-(5800 \pm 700)/(RT)],$$

$$(\alpha_{CO_2} + \alpha_{CO})_2 = 2.9 \cdot 10^{2} \cdot \exp[-(6300 \pm 700)/(RT)].$$

The amounts of CO_2 and of the (CO_2 + CO) mixture are higher in the case of compound **2** than in the thermal destruction of **1**, and the yields of H_2 and CO evolved at the end of the decomposition also increase as T_{exp} increases. For example, for **1**: α_{H_2} = 0.04 at 340 °C and 0.10 at 390 °C, α_{CO} = 0 at 340 °C, and 0.25 at 390 °C; for **2**: α_{H_2} = 0.08 at 340 °C and 0.020 at 390 °C, α_{CO} = 0.07 at 340 °C, and 0.29 at 390 °C. However, the degree of gas evolution is noticeably lower for these gases than for CO_2.

Solid products of transformations. It is shown that samples **1** and **2** are dispersed; the specific surface area of **1** $(S^0_{sp})_1$ is 9.0 m^2 g^{-1}, while $(S^0_{sp})_2$ = 8.1 m^2 g^{-1}. Broad absorption bands (AB) related to the stretching vibrations of the H—O bond of coordinated water (3000 to 3600 cm^{-1}) and the stretching vibrations of the H—C bond of the CH_2CHCOO^- anion (2900 to 3050 cm^{-1}) are observed in the IR spectra of cocrystallizates **1** and **2** (Table 1), and the system of lines in the 1300±600 cm^{-1} range is caused by the stretching vibrations of the COO groups.[7–9] Taking into account the character of the change in I_{rel} on going from **1** to **2**, a comparison of the absorption in this range with the IR spectra of compounds **3** (see Ref. 3) and **4** (see Ref. 1) allows one to assign the splitting of the AB of the stretching vibrations of the COO groups to the nature of the metal coordinated with the carboxyl groups (see Table 1). It should be noted that the absorption maxima of ν(COO) are somewhat shifted toward the low-frequency range as compared with the corresponding AB of individual compounds **3** and **4**.

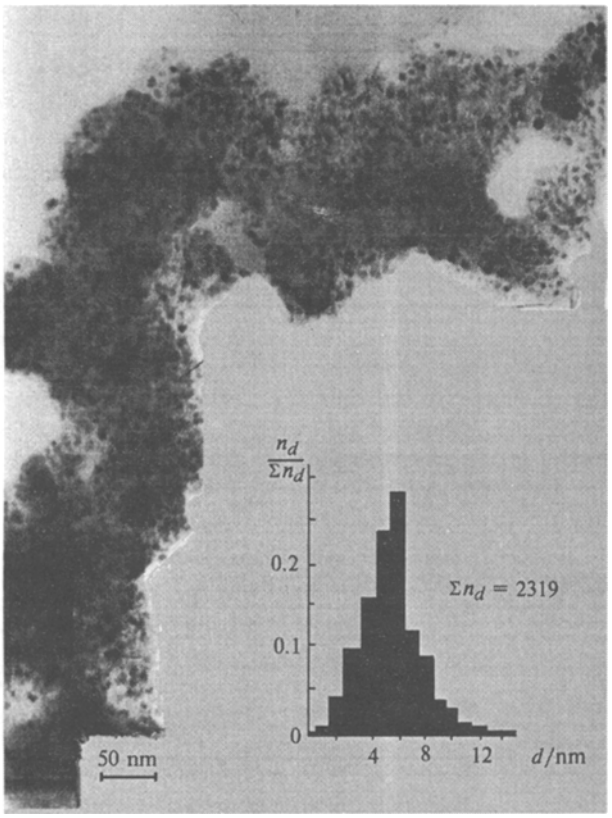

Fig. 2. Electron microscopic photograph of the decomposition product of cocrystallizate **2** at 370 °C.

The following changes in the IR spectra are observed as the degree of conversion increases: the absorption related to the stretching and bending vibrations of H_2O and the vibrations of the M←OH_2 bond disappears, which attests to the dehydration of cocrystallizates **1** and **2**; the AB at ~1630 cm^{-1} shifts toward the high-frequency region and its I_{rel} simultaneously decreases, which may be caused by the appearance of the stretching vibrations of the conjugated C=C groups;[7] I_{rel} changes for the ν_{as} and ν_s vibrations of the COO groups: I_{rel} increases as the degree of conversion increases and the intensity of the background absorption decreases due to a decrease in the consumption of the carboxyl groups, which may be related to the appearance of absorption in this range due to the formation of a system of conjugated C=C bonds; the AB at 725 and 963 to 1130 cm^{-1} related to $\rho_w(CH_2)$, ν(C=C), and πCH (—CH=CH_2) disappear; absorption at 855 cm^{-1} appears for which I_{rel} increases as the degree of conversion increases, which may be related to the appearance of δ(CH) vibrations of the —CH=CH— fragments.[7]

Thus, the analysis of the IR spectra of the solid phase in the course of the transformation indicates that the Fe and Co fragments are dehydrated and decompose.

The data of the optical microscopic (OM) studies testify that samples **1** and **2** are morphologically similar both before and after their transformation. Initial compounds **1** and **2** are light brown transparent crystals with irregular shapes (their average sizes are ~5.0 μm for **1** and 10 to 15 μm for **2** and the size distributions are fairly narrow) that form agglomerates 100 to 150 μm in size, some of which reach ~1 to 2 mm.

In the transformation of cocrystallizates **1** and **2**, slight increases in the specific surface areas are observed, which reach 13.6 and 11.3 $m^2\ g^{-1}$, respectively, by the end of their decomposition.

According to the data of the OM observations, the aggregates are enlarged in the course of the transformation. They are brittle porous formations consisting of glass-like plates (~100 μm). The transparency of these plates decreases continuously from light brown to dark brown. This indicates that the transformations of cocrystallizates **1** and **2** are voluminous, homogeneous, and similar to that observed previously[3] for compound **3**. At the end of the transformation, the sizes of the agglomerates decrease. They consist of irregular brittle plates, which break up into fragments of fine particles (~1.0 to 2.0 μm) under mechanical action. These particles are black in reflected light.

The electron microscopic (EM) studies (Fig. 2) of the final products of the decomposition of cocrystallizates **1** and **2** show that they are characterized by morphologically identical patterns: electron-contrasting nearly spherical particles with a narrow size distribution and an average diameter d = 6 nm are arranged rather uniformly (on the average, at a distance of ~8.0 nm one from another) in a less electron-contrasting matrix. They exist both as individual particles and as aggregates of three to six particles (see Fig. 2), and the fraction of these aggregates is ~50 % of the total mass of all particles.

The products of the decomposition of compounds **1** and **2** are ferromagnetic. For the product of the decomposition of **1**, magnetization (σ_s), coercivity (H_c), specific magnetic susceptibility (χ_σ), and the rectangular coefficient (j_r) are determined at 291 K: σ_s = 24.2 G $cm^3\ g^{-1}$, H_c = 625 Oe, $\chi_\sigma = 41.2 \cdot 10^{-5}\ cm^3\ g^{-1}$, j_r = 0.31. The ferromagnetic phase possesses high magnetic anisotropy at 77 K, and the magnetic fields used (±10 kOe) make it possible to measure only a particular hysteresis loop of the sample, which indicates the existence of a dispersed $CoFe_2O_4$ phase. The ferromagnetic particles contain ~50 % Fe and Co atoms, which is somewhat lower than that in the ferromagnetic phase of the product of the transformation of iron acrylate **3**, whose magnetic anisotropy at 77 K is nearly threefold lower. The remaining Fe and Co atoms form a weak magnetic phase. Probably this anisotropy is caused by exchange interaction on the interface between the ferromagnetic and antiferromagnetic phases. It is likely that CoO is the antiferromagnetic phase.

Structures of compounds 1 and 2. The mixed iron and cobalt acrylate prepared by the coprecipitation of salts **3** and **4** is probably a metallocluster monomer

Table 1. Frequencies of stretching vibrations* in the IR absorption spectra of cocrystallizates **1** and **2** and the products of the transformation of compound **1** at 360 °C ($I_{rel} = \Delta_\nu/\Delta_\nu^{max}$ is the relative intensity, Δ_ν is the absorption at frequency ν)

Initial compounds					Products of transformation of **1**						
1		**2**		Assignment	Δm = 27.8 %		Δm = 38.0 %		Δm = 48.8 %		Assignment
ν/cm^{-1}	I_{rel}	ν/cm^{-1}	I_{rel}		ν/cm^{-1}	I_{rel}	ν/cm^{-1}	I_{rel}	ν/cm^{-1}	I_{rel}	
3000—3600 br		3000—3600 br		ν(OH) (H_2O)							
3045		3045		ν_{as}(CH)							
2990		2960		ν_s(CH)	2930						ν(CH)
1628	0.575	1630	0.74	ν(C=C), δ(OH)(H_2O)	1640	0.35	1680	0.46	1685	0.38	ν(C=C)
1572	1.00	1575	1.00	ν_{as}(COO) (Fe cluster)	1555	1.00	1555	1.00	1565	1.00	ν_{as}(COO) (Fe cluster)
1540	0.75	1540	0.80	ν_{as}(COO) (Co)	1540	0.99	1540	0.99	1550	1.07	ν_{as}(COO) (Co)
1520	0.75	1525	0.77	ν_{as}(COO) (Fe cluster)	1520	0.92	1520	0.98	1520	0.99	ν_{as}(COO) (Fe cluster)
1505	0.475	1505	0.485	ν_{as}(COO) (Co)	1505 sh	0.715	1498	0.89			ν_{as}(COO) (Co)
1492	0.44	1490 sh	0.39	δ(CH)	1490	0.6					δ(CH)
1435	0.845	1435	0.92	ν_s(COO) (Fe cluster)	1435	0.85	1440	1.02	1420	1.23	ν_s(COO) (Fe cluster), $\delta(OH_2)$ (—CH_2—CHR—)
1420	0.785	1420	0.92	ν_s(COO) (Co)	1415	0.85	1408	1.07			ν_s(COO) (Co), $\delta(OH_2)$ (H_2C—CR—)
1360	0.735	1360	0.82	ν_s(COO) (Fe cluster)	1400	0.97	1395	1.10	1400	1.20	ν_s(COO) (Fe cluster), $\delta(OH_2)$ (CH_2=CR—)
1350	0.82	1350	0.71		1315	0.57					ν_s(COO) (Co), δ(OH) (—CH_2—CHR—)
1270	0.51	1270	0.44	$\rho_t(CH_2)$	1280 sh	0.51	1270 sh	0.665	1265	1.08	$\rho_t(CH_2)$ (—CH_2—CH=CH—)$_{trans}$
					1185	0.35	1160		1150	1.37	ν(C—C) (=CH—CHR—)
1130	0.05	1120 br	0.10								
1068	0.31	1068	0.32	ν(C—C)							
990	0.39	990	0.38	π(CH) (—CH=CH_2)							
965	0.31	965	0.31	π(CH) (—CH=CH_2)							
910	0.08	910	0.07	ρ(OH) (H_2O), ν(M—OH_2)	855	0.08	860	0.15	875	0.33	δ(CH) (—CH=CHR)
830	0.61	830	0.61	$\rho_w(CH_2)$	835	0.09	830	0.10	830	0.20	ρ_w(CH) (—CH_2—CHR—)
725	0.185	728	0.12		775	0.07	755	0.11	750	1.11	
677	0.40	673	0.50	$\rho_r(CH_2)$, δ(M—OH_2)	645 br	0.03					ρ_t(CH) (—CH_2—CR=CH—)$_{cis}$
598	0.185	598	0.11	$\delta(CH_2)$, δ(M—OH_2)	592	0.02					$\delta(CH_2)$, ρ_w(CH) (—CH=CHR)
547	0.14	545	0.07	$\delta(CH_2)$, δ(M—OH_2)							

* The following designations for vibrations are used: ν, stretching; δ, bending; ρ_w, wagging; ρ_r, rocking; ρ_t, twisting; π, extraplanar; as, asymmetric; s, symmetric; sh, shoulder; br, broad.

including two different metallocarboxylate fragments. One of them, the Fe-containing fragment, is a trinuclear cluster of the iron acrylate μ_3-oxo complex.[3,11] According to the X-ray analysis data,[12,13] its structure is a regular triangle with the O atom in the centerand the Fe atoms at the vertices ($R_{Fe-Fe} \approx 3.27$ to 3.30 Å)[12] united by a pair of bidentate carboxylate (acrylate) groups. Bonding between the Fe atoms and H_2O (in **3**) or other donating ligands results in the formation of the octahedral coordination characteristic of the Fe atoms. The

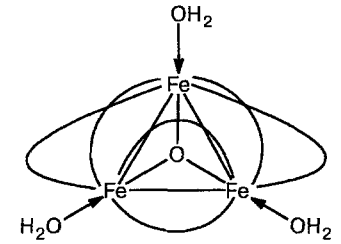

measurements of the magnetic susceptibility of compound **3** confirm the proximity of the Fe atoms to one other in this structure. The paramagnetic susceptibility of salt **3** is lower than the susceptibility expected assuming that the Fe atoms exist as "separate" Fe^{3+} ions ($3d^5$—^6S) with $s = 5/2$ and $g = 2$. For example, χ_σ is equal to $1.75 \cdot 10^{-5}$ cm^3 g^{-1} at 291 K and $3.22 \cdot 10^{-5}$ cm^3 g^{-1} at 77 K (calculated values for these temperatures are $6.62 \cdot 10^{-5}$ and $25 \cdot 10^{-5}$ cm^3 g^{-1}, respectively). It should be mentioned that the study of the change in the ESR signal with $g = 2$ with the variation of temperature makes it possible to say that there is a violation of Hund's rule for the Fe^{3+} ion in **3**. One of the possible reasons for this may be suppression of the intraatomic exchange interaction due to the close arrangement of the adjacent Fe^{3+} ions.

The paramagnetic susceptibility of salt **4** is close to the calculated value. Assuming that the Co atoms in molecule **4** exist as non-interacting Co^{2+} ions ($3d^7$—^4F) with $s = 3/2$ and $g = 2$, the calculated values of χ_σ are equal to $4.83 \cdot 10^{-5}$ cm^3 g^{-1} ($2.93 \cdot 10^{-5}$ cm^3 g^{-1} at 291 K and $11.1 \cdot 10^{-5}$ cm^3 g^{-1} at 77 K). The experimental values are $4.83 \cdot 10^{-5}$ and $15.1 \cdot 10^{-5}$ cm^3 g^{-1}, respectively. At present it is difficult to judge the structure of compound **4**: there is little data on the stereochemistry of cobalt carboxylates.[12,13] It is likely that the acrylate groups in $Co(CH_2CHCOO)_2 \cdot H_2O$ can be either monodentate or bidentate ligands.[12] This is confirmed indirectly by the IR absorption spectra of **4**, in which a system of lines is observed in the range of the asymmetric vibrations of COO groups.[1] The Co atom is coordinated to the H_2O molecule to form tetrahedral coordination, which is typical of known cobalt carboxylates along with octahedral coordination.[12,13]

It can be assumed that the peculiarities of the coordination of Fe^{3+} and Co^{2+} are retained in cocrystallizates **1** and **2**. For example, using the $\chi_\sigma(Fe^{3+})$ and $\chi_\sigma(Co^{2+})$ values obtained for salts **3** and **4**, it can be expected that for **1** $\chi_\sigma = 3.17 \cdot 10^{-5}$ cm^3 g^{-1} at 291 K and $8.63 \cdot 10^{-5}$ cm^3 g^{-1} at 77 K. These values are close to the values observed experimentally: $2.73 \cdot 10^{-5}$ and $6.5 \cdot 10^{-5}$ cm^3 g^{-1}, respectively. It is possible that when there are no molecules of water of crystallization in cluster **1** and when their number is small in **2**, acrylate groups can play the role of H_2O to achieve the same coordination of Fe^{3+} and Co^{2+} as in salts **3** and **4**. Some of these acrylate groups become tridentate (as occurs in the dehydration of crystal hydrates of carboxylates of transition metals),[12] which in turn can result in a change in the strengths of the C—O bonds. It is likely that this is one of the reasons for the shift in the AB of the stretching vibrations of the COO groups to the low-frequency region in the IR spectra of cocrystallizates **1** and **2** as compared to the spectra of **3** and **4** (see above).

Routes of transformation of cocrystallizates 1 and 2. The routes of the thermal transformations of compounds **1** and **2** should be primarily determined by the thermal stability of the metallocarboxylate groups and their ability to eliminate an acrylate radical. It has been shown for Fe^{3+} cluster **3** that the H_2O—Fe bonds are the weakest and the Fe—O bonds with carboxylate ligands, including acrylates, are energetically unequal.[3,11,13,14] It is likely that the Co—O bonds in the dehydrated Co-acrylate fragments are also energetically unequal, because the dentate character of the acrylate groups changes due to dehydration.

Starting from the above considerations, it can be concluded that the initial stages of the thermal transformations of cocrystallizates **1** and **2** are dehydration followed by the formation of $CH_2CHCOO^\cdot$ radicals due to cleavage of the M—O bond (M is a metal). The reactions of these radicals with the acrylate metal-containing fragments result in the formation of acrylic acid and the radical $R^\cdot$ whose acrylate group is depleted in hydrogen

$$CH_2CHCOO^\cdot + HR \longrightarrow CH_2CHCOOH + R^\cdot ,$$

where $R^\cdot = CHCHCOO^\cdot R^1$ and R^1 is the metallocarboxylate fragment.

In its turn, radical $R^\cdot$ initiates the process of copolymerization, and decarboxylation of the metal-containing groups occurs in the polymer formed, which depends on T_{exp}.

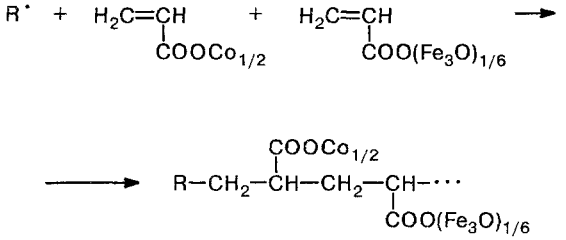

Writing the compositions of cocrystallizates **1** and **2** as $MO_{0.5(1-x)}(CH_2CHCOO)_2(H_2O)_{y+(1-x)/6}$, where M = Co_xFe_{1-x} (for **1**: $x = 0.46$, $y = 0$; for **2**: $x = 0.337$, $y = 0.64$) and taking into account the acrylate groups depleted in hydrogen (CHCHCOO), the process of the thermal transformation of cocrystallizates **1** and **2** can be presented as in Scheme 1.

Scheme 1

$$MO_{(1-x)/2}(CH_2CHCOO)_2(H_2O)_{y+(1-x)/6} \xrightarrow[-[y+(1-x)/6]H_2O]{\text{Dehydration}} MO_{(1-x)/2}(CH_2CHCOO)_2 \xrightarrow[-\beta CH_2CHCOOH]{\text{Copolymerization}}$$

$$\longrightarrow MO_{(1-x)/2}(CH_2CHCOO)_{2-\beta}(CHCHCOO)_\beta \xrightarrow[-(p+q)/2\ MO_{(1-x)/2}]{\text{Decarboxylation}\ -(p+q)\ CO_2,}$$

$$\longrightarrow (MO_{(1-x)/2})_{1-(p+q)/2}(CH_2CHCOO)_{2-\beta-p}(CH_2CH)_p(CHCHCOO)_{\beta-q}(CHCH)_q$$

As mentioned above, the formation of CO_2, $CH_2CHCOOH$, H_2O, H_2, and CO is confirmed by the IR spectra and the data of mass spectrometry. The appearance of H_2 and CO in the transformation products seems to be caused by the oxidation of M or its oxide:

$$MO_a + fCO_2 \longrightarrow MO_{a+f} + fCO\ ,$$

$$MO_b + gH_2O \longrightarrow MO_{b+g} + gH_2\ .$$

The reaction between Fe and Co oxides can result in the formation of cobalt ferrite, $CoFe_2O_4$.

On the basis of the scheme presented above, the following system of mass balance equations can be written for α_i:

$$\begin{cases} \alpha_{CO_2} + \alpha_{CO} + 3\alpha_{CH_2CHCOOH} + 3\alpha_{CH_2CHCOO} + \\ \quad + 3\alpha_{CHCHCOO} + 2\alpha_{CH_2CH} + 2\alpha_{CHCH} = 6 \\ \alpha_{H_2} + \alpha_{H_2O} + 2\alpha_{CH_2CHCOOH} + 1.5\alpha_{CH_2CHCOO} + \\ \quad + \alpha_{CHCHCOO} + 1.5\alpha_{CH_2CH} + \alpha_{CHCH} = 3 + y + (1-x)/6 \\ 2\alpha_{CO_2} + \alpha_{CO} + \alpha_{H_2O} + 2\alpha_{CH_2CHCOOH} + 2\alpha_{CH_2CHCOO} + \\ \quad + 2\alpha_{CHCHCOO} + \lambda\alpha_{MO_\lambda} = 4 + (1-x)/2 + y + (1-x)/6 \\ \alpha_M + \alpha_{MO_\lambda} = 1 \\ \Delta m/\pi_0 = MM_{H_2}\alpha_{H_2} + MM_{H_2O}\alpha_{H_2O} + MM_{CO}\alpha_{CO} + \\ \quad + MM_{CO_2}\alpha_{CO_2} + MM_{CH_2CHCOOH}\alpha_{CH_2CHCOOH} \\ m_t/\pi_0 = (m_0 - \Delta m)/\pi_0 = MM_M\alpha_M + MM_{MO_\lambda}\alpha_{MO_\lambda} + \\ \quad + MM_{CH_2CHCOO}\alpha_{CH_2CHCOO} + MM_{CH_2CH}\alpha_{CH_2CH} + \\ \quad + MM_{CHCHCOO}\alpha_{CHCHCOO} + MM_{CHCH}\alpha_{CHCH} \end{cases}$$

Here MM_i is the molecular mass of the i-th substance or fragment, $MO_\lambda = Co_zFe_{1-z}O_\lambda$ is the overall expression for the oxide phase (in the case of $CoFe_2O_4$, $z = 0.333$, $\lambda = 1.333$).

The solution of this system allows one to calculate the composition of the products in the course of the thermal decomposition and at the end of the transformation (Eqs. (1)—(6)) based on quantitative data from the mass spectral determination of CO_2, CO, and H_2 ($\alpha_{CO_2} = n$, $\alpha_{CO} = p$, $\alpha_{H_2} = 1$), the total gas evolution (α^Σ), and the mass loss of the sample (Δm).

$$\alpha_{CH_2CHCOOH} = \frac{1}{72}\left[\frac{\Delta m}{\pi_0} - 18\alpha^0_{H_2O} - 28m - 44(n-1)\right] \quad (1)$$

$$\left(\alpha^0_{H_2O} = y + (1-x)/6\right)$$

$$\alpha_{CHCHCOO} + \alpha_{CHCH} = \alpha_{CH_2CHCOOH} \quad (2)$$

$$\alpha_{CH_2CHCOO} + \alpha_{CH_2CH} = 2(1-\alpha_{CH_2CHCOOH}) \quad (3)$$

$$\alpha_{CH_2CH} + \alpha_{CHCH} = n + p \quad (4)$$

$$\alpha_{H_2O} = \alpha^0_{H_2O} - 1 \quad (5)$$

$$\lambda\alpha_{MO_\lambda} = p + 1 + 0.5(1-x) \quad (6)$$

At the end of the transformation $\alpha_{MO_\lambda} = 1$. Assuming that all of the oxygen in MO_λ is concentrated in $CoFe_2O_4$, one can calculate the maximum possible experimental value of $\alpha_{CoFe_2O_4} = (1/4)\lambda$ and the yield of $CoFe_2O_4$ relative to the theoretical yields for cocrystallizates **1** and **2**: $\xi_{CoFe_2O_4} = 0.5\lambda/(1-x)$.

The accumulation of products during the increase in the degree of gas evolution, $\eta = \alpha_t^\Sigma/\alpha_\infty^\Sigma$ (see Fig. 1), for **1** and **2** is characterized by the following general regularities: the main fraction of $CH_2CHCOOH$ is evolved during heating and a smaller amount is liberated in the course of the further transformation (Fig. 3, t_1, curves *4*); a portion of the products evolved is condensed, which follows from a comparison of the value of $\eta_{\Delta\alpha}$ with the mass loss of the sample, $\eta_{\Delta m} = \Delta m_t/\Delta m_\infty$ (see Fig. 3, curve *7*), and is observed experimentally by the formation of dew on the parts of the reaction vessel whose temperature is ~20 °C (H_2O, $CH_2CHCOOH$); only CO_2, $CH_2CHCOOH$, and H_2O are formed during heating of the sample ($\sim t_1$), and $\alpha_{CO_2} > \alpha_{CH_2CHCOOH}$ for **1** and $\alpha_{CO_2} < \alpha_{CH_2CHCOOH}$ for **2**; H_2 and CO appear in the main gas evolution process (after t_1), and $\alpha_{CO_2} \gg \alpha_{H_2} + \alpha_{CO}$; the amount of H_2O in the case of

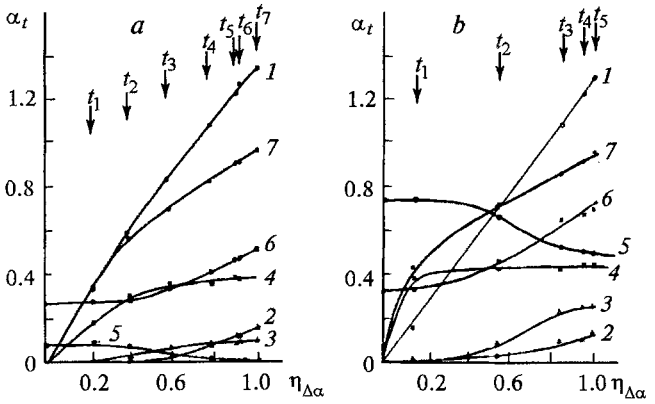

Fig. 3. Kinetics of the accumulation of gaseous products. *a*. Cocrystallizate **1**, *t*/min: t_1 = 20, t_2 = 100, t_3 = 350, t_4 = 540, t_5 = 962, t_6 = 990, t_7 = 1380; T_{exp} = 360 °C. *b*. Cocrystallizate **2**, *t*/min: t_1 = 2.5, t_2 = 100, t_3 = 340, t_4 = 560, t_5 = 840; T_{exp} = 370 °C. Curves: *1*, α_{CO_2}; *2*, α_{CO}; *3*, α_{H_2}; *4*, $\alpha_{CH_2CHCOOH} = \alpha_{CHCHCOO} + \alpha_{CHCH}$; *5*, α_{H_2O}; *6*, $\lambda\alpha_{MeO_\lambda}$; *7*, $\eta_{\Delta m}$.

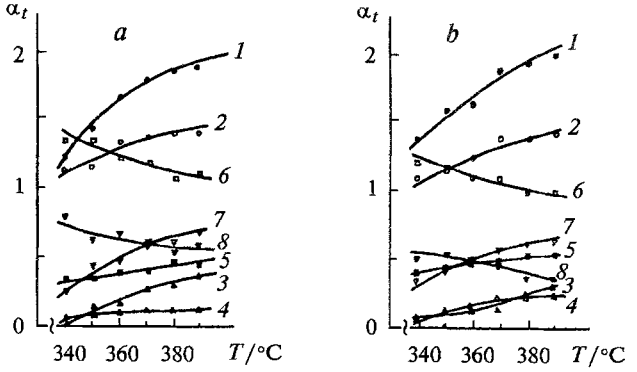

Fig. 4. Dependence of the yield of the transformation of the products on T_{exp}.
a. Cocrystallizate **1**, $m_0/V = 1.28 \cdot 10^{-3}$ g cm^{-3}.
b. Cocrystallizate **2**, $m_0/V = 1.80(\pm 0.05) \cdot 10^{-3}$ g cm^{-3}. Curves: *1*, α_f^{Σ}; *2*, α_{CO_2}; *3*, α_{CO}; *4*, α_{H_2}; *5*, $\alpha_{CH_2CHCOOH} = \alpha_{CH_2CHCOO} + \alpha_{CHCH}$; *6*, $\alpha_{CH_2CHCOO} + \alpha_{CH_2CH}$; *7*, $\xi_{CoFe_2O_4}$; *8*, $2\gamma \cdot 10^{-1}$.

cocrystallizate **2** (see Fig. 3, curve *5*) decreases as the transformation occurs.

The product yield at the end of the transformation (Fig. 4) depends on T_{exp}. When T_{exp} increases, α_{CO_2}, α_{CO}, α_{H_2}, and $\alpha_{CH_2CHCOOH}$ also increase, and α_{CO_2} (**1**) $\cong \alpha_{CO_2}$(**2**). At the same time, $\alpha_{CO_2} > \alpha_{H_2} + \alpha_{CO} + \alpha_{CH_2CHCOOH}$ and $\alpha_{CH_2CHCOOH} > \alpha_{H_2}$, α_{CO}. In the products of the transformation of **2**, $\alpha_{CO} \approx \alpha_{H_2}$, and in the case of **1**, $\alpha_{CO} > \alpha_{H_2}$, which is probably related to the absence of the crystallization water in **1**. The level of the evolution of $CH_2CHCOOH$ as well as the amount of $CoFe_2O_4$ are somewhat higher in the products of the transformation of cocrystallizate **2** than in those of **1**. However, $\xi_{CoFe_2O_4}$ (see Fig. 4, curve *7*) for **1** exceeds $\xi_{CoFe_2O_4}$ for **2**. For cocrystallizate **1**, the value of $\xi_{CoFe_2O_4}$ at 360 °C ($\xi_{CoFe_2O_4}$ = 0.48) coincides with that estimated from the results of the magnetic measurements (see above).

The $\gamma = (\alpha_{CH_2CHCOO} + \alpha_{CH_2CH})/(\alpha_{CHCHCOO} + \alpha_{CHCH})$ value is a very significant characteristic of thermal decomposition. At the end of the transformation, this value characterizes the chain length (2γ) of the polymer formed: it is the ratio of the terminal acrylate groups depleted in hydrogen to the number of acrylate groups inside the polymer chain. The value $2\gamma = \psi$ decreases as T_{exp} increases:

$$\psi = 1.7 \cdot 10^{-2} \exp\left(\frac{4600 \pm 500}{RT}\right) \text{ for } \mathbf{1}$$

and

$$\psi = 4.8 \cdot 10^{-3} \exp\left(\frac{6500 \pm 500}{RT}\right) \text{ for } \mathbf{2}.$$

The ψ values for cocrystallizate **1** range from 7.7 (340 °C) to 5.0 (390 °C) and they are higher than those for **2**: from 5.5 (340 °C) to 3.8 (390 °C). Therefore, an increase in the relative content of the Fe cluster fragments in **2** results in a decrease in ψ. At the same time, the values of ψ for cocrystallizates **1** and **2** are intermediate between the ψ values corresponding to this temperature range in the thermal transformation of **3** (5.3 (330 °C) to 2.8 (370 °C))[3] and **4** (11.6 (350 °C) to 1.5 (390 °C)).[1] This allows us to assume that the formation of the $CH_2CHCOO^{\cdot}$ radical from **3** plays the main role in the initiation of the copolymerization of salts **3** and **4**. Compound **3** is an Fe-containing cluster monomer for which the energetic non-equality of the Fe—O bonds and the possibility of elimination at 340 to 390 °C to form two CH_2CHCOO groups per one dehydrated $(FeO_{0.5})_3(CH_2CHCOO)_6$ fragment have been established.[3,11] Therefore, an increase in its relative content in cocrystallizate **2** results in an increase in the yields of $CH_2CHCOO^{\cdot}$ radicals and $CH_2CHCOOH$ and, hence, in a decrease in ψ, which is observed experimentally. In this connection, Co-containing fragments are less reactive, which is indicated by the ψ values during the thermal decomposition of salt **4**.

The subsequent thermal transformations of cocrystallizates **1** and **2** are related to the decarboxylation of the metal-containing acrylate fragments in the copolymer formed (which mainly determines the observed kinetics of gas evolution), in particular, to the thermal stability of the terminal CHCHCOO groups depleted in hydrogen and the intrachain CH_2CHCOO groups. It has previously been shown for salts **3** and **4** that the thermal stability of terminal metallocarboxylate groups is lower than that of intrachain groups, and in **3** this difference results in the appearance of two temperature ranges of gas evolution.[1,3] In the case of cocrystallizates **1** and **2**, when the formal kinetic parameters of gas evolution are similar, there is a characteristic change in the level of $\eta_{1\infty}$ on going from **1** to **2**. This can be explained by

assuming that the thermal stabilities of the Co- and Fe-containing fragments in the copolymer formed are different. According to this assumption, the Co-containing radical initiates the copolymerization, and the thermal stability of the Co-containing terminal and intrachain fragments is lower than that of the Fe-containing fragments, which are mainly intrachain. Then an increase in the fraction of the more stable Fe-containing fragments and, hence, a decrease in $\eta_{1\infty}$ take place on going from cocrystallizate **1** to **2**. The values of $\eta_{1\infty}$ obtained in the description of the kinetics of gas evolution for **1** and **2** (see Fig. 1) and the values of $\eta_{1\infty}$ calculated from the yield of $CH_2CHCOOH$ in terms of the assumption mentioned above are presented in Table 2. The calculated values of $\eta_{1\infty}$ and those determined from the kinetic measurements of gas evolution agree satisfactorily. It should be noted that the data on the changes in the magnetic parameters of the products of the transformation of **1** at 360 °C testify in favor of the higher stability of the Fe-containing fragments: strong changes in σ, H_c, and χ_σ are observed at the end of the transformation when the decarboxylation of the Fe-containing fragments occurs.

Thus, the thermal transformations of cocrystallizates **1** and **2** at 340 to 390 °C include three main processes: dehydration, the combination of the thermal decomposition of monomers with their radical homopolymerization and copolymerization, and decarboxylation to form an oxide phase, whose main component is cobalt ferrite. The solid-phase product of the transformations of clusters **1** and **2** is made up of nanometer-sized particles of complex oxides stabilized in the polymer matrix. The analysis of the kinetics of gas evolution and the appearance of acrylic acid at the end of the transformation of cocrystallizates **1** and **2** allow us to draw the conclusion that the Fe cluster and Co-containing fragments have a mutual effect on the process of thermal transformation that manifests itself in the initiation of the polymerization processes due to the partial thermal destruction of the Fe cluster monomer and the decreased thermal stability of the Co-containing fragments in the polymer formed.

Table 2. Comparison of experimental and calculated values of $\eta_{1\infty}$

Cocrystallizate	Parameter		
	T/°C	$\eta_{1\infty}$ (exp.)	$\eta_{1\infty}$ (calcd.)
1	340	0.65	0.62
	350	0.60	0.57
	360	0.45	0.42
	370	0.45	0.40
	380	0.40	0.37
	390	0.40	0.36
2	340	0.50	0.44
	350	0.40	0.39
	360	0.40	0.36
	370	0.35	0.32
	380	0.35	0.31
	390	0.35	0.29

At the same time, some problems remain unsolved and could be the object of further studies. In particular, the following questions are important for the elucidation of the stability of the copolymer formed and the possibility of the formation of complex oxides in the course of the decarboxylation of metallocarboxylate groups: the inclusion of metallocluster groups into a copolymer, the retention of their structures in the process of polymerization, the regularity of distribution in the chain of metallocarboxylate groups (block, statistical, or alternating), and the mechanism of the decarboxylation of complex cluster fragments.

Experimental

Cocrystallizates **1** and **2** were prepared by coprecipitation of salts **3** and **4** from an alcoholic solution at Fe/Co ratio of 1 : 1 and 2 : 1, respectively. For **1**: found (%): Fe, 15.4; Co, 13.7. $[Fe_3O(CH_2CHCOO)_6OH] \cdot [Co(CH_2CHCOO)_2]_{2.4}$. Calculated (%): Fe, 14.69; Co, 13.2. For **2**: found (%): Fe, 17.0; Co, 9.1. $[Fe_3O(CH_2CHCOO)_6OH] \cdot [Co(CH_2CHCOO)_2]_{1.5} \cdot 3H_2O$. Calculated (%): Fe, 17.08; Co, 9.12. The Fe/Co ratio = 1.17 (**1**) and 1.98 (**2**).

Thermal transformations of cocrystallizates **1** and **2** in a self-generating atmosphere and under static non-isothermic conditions were studied at T_{exp} = 340 to 390 °C and m_0/V = $(0.61-1.85) \cdot 10^{-3}$ g cm^{-3}. The volume of the heated tube did not exceed $0.05V$. The kinetics of gas evolution were recorded using a membrane zero-manometer. The mass loss of the sample and the amounts of gaseous products at ~20 °C and those condensing at 77 K were determined at the end of the experiments.

The specific surface areas of the initial samples and the solid-phase products of their thermal transformation were determined by the low-temperature nitrogen adsorption (BET) method[15]. IR absorption spectra of gaseous and condensed products were recorded on an UR-10 instrument from 400 to 4000 cm^{-1}. Solid samples were prepared as a fine dispersed powder between NaCl or KBr glasses, as a suspension in CCl_4, and as pellets with KBr. Optical microscopic observations were performed in transmitted light on MBI-15 Leitz Metalloplan instruments. An IEM-1200Ex instrument (accelerating voltage 120 kV) was used for electron microscopic studies. Samples were prepared as a suspension of a powdered substance in ethanol, which then was deposited on a carbon film-substrate. Mass spectral analysis was performed on an MS 3702 quadrupole mass-spectrometer. Magnetic measurements were carried out on a PAR-155 vibration magnetometer.

The authors are grateful to A. N. Titkov for optical microscopic and electron microscopic studies.

References

1. E. I. Aleksandrova, G. I. Dzhardimalieva, A. S. Rozenberg, and A. D. Pomogailo, *Izv. Akad. Nauk, Ser. Khim.*, 1993, 308 [*Russ. Chem. Bull.*, 1993, **42**, 264 (Engl. Transl.)].
2. E. I. Aleksandrova, G. I. Dzhardimalieva, A. S. Rozenberg, and A. D. Pomogailo, *Izv. Akad. Nauk, Ser. Khim.*, 1993, 303 [*Russ. Chem. Bull.*, 1993, **42**, 259 (Engl. Transl.)].

3. A. S. Rozenberg, E. I. Aleksandrova, G. I. Dzhardimalieva, A. N. Titkov, and A. D. Pomogailo, *Izv. Akad. Nauk, Ser. Khim.*, 1993, 1743 [*Russ. Chem. Bull.*, 1993, **42**, 1666 (Engl. Transl.)].
4. S. P. Gubin and I. D. Kosobudskii, *Usp. Khim.*, 1983, **52**, 1350 [*Russ. Chem. Rev.*, 1983, **52** (Engl. Transl.)].
5. S. P. Gubin, *Zh. Vses. Khim. Obshch. im. D. I. Mendeleeva*, 1987, **32**, 3 [*Mendeleev Chem. J.*, 1987, **32** (Engl. Transl.)].
6. G. V. Lisichkin and V. F. Petrunin, *Zh. Vses. Khim. Obshch. im. D. I. Mendeleeva*, 1991, **36**, 131 [*Mendeleev Chem. J.*, 1991, **36** (Engl. Transl.)].
7. A. A. Babushkin, P. A. Bazhulin, F. A. Korolev, L. V. Levshin, V. K. Prokof'ev, and A. P. Striganov, *Metody spektral'nogo analiza* [*Methods of Spectral Analysis*], Izd. Mosc. Univ., Moscow, 1962 (in Russian).
8. K. Nakamoto, *Infrared and Raman Spectra of Inorganic and Coordination Compounds*, Wiley & Sons, New York, 1962.
9. P. H. McCuskey, R. L. Suyder, and R. A. Coudrate, *J. Sol. State Chem.*, 1989, **83**, 332.
10. L. I. Mirkin, *Spravochnik po rentgenostrukturnomu analizu polikristallov* [*A Handbook of X-ray Diffraction Analysis of Polycrystals*], Fizmatgiz, Moscow, 1961 (in Russian).
11. Yu. M. Shul'ga, O. S. Roshchupkina, G. I. Dzhardimalieva, I. V. Chernushevich, A. F. Dodonov, Yu. V. Baldokhin, P. Ya. Kolotyrkin, A. S. Rozenberg, and A. D. Pomogailo, *Izv. Akad. Nauk, Ser. Khim.*, 1993, 1739 [*Russ. Chem. Bull.*, 1993, **42**, 1661 (Engl. Transl.)].
12. M. A. Porai-Koshits, in *Kristallokhimiya, Itogi Nauki i Tekhniki* [*Crystal Chemistry, Results of Science and Technique*], VINITI AN SSSR, Moscow, 1981, **15**, 13 (in Russian).
13. R. C. Mehrotra and R. Bohra, *Metal Carboxylates*, Acad. Press, London—New—York, 1983.
14. A. van den Bergen, R. Colton, and M. Perey, *Inorg. Chem.*, 1993, **32**, 3408.
15. S. J. Gregg and K. S. W. Sing, *Adsorption, Surface Area, and Porosity*, Academic Press, New York, 1967.

Received May 10, 1994;
in revised form October 28, 1994